

187. Preliminary Results from the ROTATE-2013 Season

Joshua Wurman, Karen Kosiba, and Paul Robinson
Center for Severe Weather Research, Boulder, Colorado

Tim Marshall
Haag Engineering

1. Introduction

During the spring of 2013, attempts were made to deploy a dual-polarization dual-frequency Doppler on Wheels (DOW) mobile radar (DOW6 hereafter) and the Rapid-Scan-DOW (RSDOW hereafter) along with in-situ Tornado Pod instrumentation near and in several violent (EF-3 or greater) tornadoes. These include the EF-3 El Reno, Oklahoma tornado (31 May), the EF-4 Bennington, Kansas tornado (date), and the EF-4 Rozel, Kansas (date) tornado.

2. The El Reno, Oklahoma tornado

During the afternoon of 31 May 2013, a discontinuous line of thunderstorms formed in western Oklahoma, from near Weatherford, extending northeast. Shortly after a cell merger/interaction at the southern edge of this convection¹, the first tornado warning was issued by the National Weather Service (NWS) at 2236 UTC (hereafter all times are UTC) on 31 May 2013, a tornado was reported at 2255 (though the tornado track posted by the NWS begins at 2303) (<http://www.srh.noaa.gov/oun>). Based on NWS and DOW data, the tornado circulation grew in both size and intensity into a large tornado / multiple-vortex mesocyclone (MVMC) which tracked generally east-southeastward, then eastward until 2318, crossing US Highway 81 (US-81) near 2319 south of El Reno, Oklahoma, then moved generally northeastward to Interstate 40 (I-40), becoming nearly stationary for several minutes, possibly looping on itself, before moving eastward along and near I-40, then becoming nearly stationary or looping again near I-40, as it dissipated at 2345² (Fig. 1).

2.1 Overview from the KTLX WSR-88D

The dual-polarization KTLX Weather Service Radar 88D (KTLX) observed a strong vortex signature after 2305 from a range of about 75km (Fig. 2). At this time, gate-to-gate shear exceeded 50m/s and there was a suggestion of a developing but barely resolvable low reflectivity eye (LRE), but no prominent debris signature (DS) in either the ZDR or r_{HV} fields. By 2315 the circulation had grown and intensified. There is a suggestion (confirmed using fine-scale resolution DOW data) of quasi-concentric wind field maxima, one with a diameter, from peak inbound to peak outbound Doppler velocity, $DX_{max}=1-2km$, the other much smaller. However, at $\sim 60km$ range, the KTLX radar has a beam width of $>1km$, and does not resolve sub-kilometer-scale features. Both ZDR and r_{HV} fields reveal lower values in the region of most intense winds, likely caused by lofted debris (Ryzhkov et al. 2005; Bluestein et al. 2007). A prominent region of high ZDR ($>2dB$), moderate reflectivity ($>45dBZ$) and high r_{HV} (>0.9) wraps around the circulation and also protrudes slightly southwestward. This signature extends north and then east-southeastward along the edge of the supercell coincident with a region of inferred inflow, similar to the observations of Kumijan (2011), who suggests that this is indicative of large drops able to fall out of the periphery of the updraft (while smaller drops are carried aloft). Low ZDR ($<1.0dBZ$) and high r_{HV} on the west side of the hook is suggestive of small drops, possibly forced downward within the rear-flank downdraft (Kumijan 2011). By 2319, the large tornado/MVMC circulation had grown and intensified further with two prominent shear/rotation signatures evident to the east and west of the center of circulation. The stronger eastern circulation was associated with a barely discernible LRE, while none is visible to the west. Both vortices are located in a region of low r_{HV} and low ZDR, but values are lower near

¹ The mechanism of tornadogenesis is beyond the scope of this paper. The role of mergers in tornadogenesis has been explored elsewhere, e.g. Wurman et al. 2007b, Hastings et al. 2012ab

² Dissipation time based on DOW observations.

the eastern one, likely because the eastern vortex/shear zone is more intense, thus lofting more debris. By 2324, a LRE is more distinct and surrounded by a debris ring echo (DRE)(low r_{HV} , low ZDR), which is approximately co-located with an inner vortex. A large region of low ZDR and r_{HV} extends for 3-5 km near the circulation center, indicative of continued, and perhaps more extensive, debris lofting. To the immediate east of the circulation, an arc of low r_{HV} connects to the near-circulation region of low r_{HV} . This arc of low r_{HV} is coincident with a large gradient in reflectivity and Doppler velocity along the knob of the hook. The tornado signature weakens by 2333 (not shown) then re-intensifies by 2338, but not to its earlier strength, before finally dissipating. At 2333 and 2338 an anticyclonic wind couplet is evident several km to the southeast of the primary tornado. At 2338 two such circulations can be seen, but DOW data (discussed below) reveal that only one of these KTLX-observed vortices at ~1km AGL is manifested as a tornado near the surface (~100m AGL).

2.2 DOW dual-polarimetric observations of the tornado

Two DOWs deployed in the path of the supercell after 2316. The dual-polarization, dual-frequency DOW6 radar collected data in the tornado from 2316-2323 at 35.4415 N, 97.7244 W and 2335-2341 at 35.4788N, 97.7775W (between, before and after these times DOW6 scanned during very short deployments and while mobile), and the RSDOW deployed from 2318-2327 at 35.4348N, 97.7776W, and from 2329-2348 at 35.4376N, 97.7775W, both documenting evolution of the most intense, complex and largest phases of the tornado.³

The DOW radars, deployed at $\frac{1}{4}$ the range of KTLX, 12-15 km from the tornado in most data presented here, with low-level updates at 15-43 times shorter intervals, allowed for the exploration of the structure and evolution of the tornado/MVMC and its internal sub-vortices at much finer temporal and spatial scale. At 2316, DOW6 revealed structures in

³ The RSDOW and DOW have 0.9 degree beam widths, sample at 50m (RSDOW) and 30-60m (DOW6) gate lengths, and scan at 50 deg/s to produce volumetric updates at 7s (RSDOW: 6 elevations) and 21s (DOW6: 3 elevations) intervals.

the tornado/MVMC similar to but in finer detail than those observed by KTLX at 2315, such as an LRE coincident with values of slightly reduced r_{HV} and low ZDR (Fig 3).⁴ The arc of high ZDR and region of low ZDR also are evident. Despite wavelength differences, and differences in observation geometry, the X-band DOW6 (3-cm radiation) and S-band (10-cm radiation) KTLX ZDR and r_{HV} fields are consistent, particularly when compared for similar times (e.g., 2319 and 2324), providing confidence in the DOW mapping of small-scale features invisible to KTLX. The better resolution of the DOW6 data reveal that, at 2316, a region of large velocities are coincident with a region of lower ZDR along the west side of the hook, perhaps suggesting an enhanced region of downward motion, as discussed above. At 2319 DOW data reveal that the high ZDR spiral, though still wrapping around to the east side of the tornado, has become diffuse, a weakened LRE persists, and two vortices exhibiting lower ZDR and moderate r_{HV} are present well to the northwest of the main tornado. DOW6 data at 2323 show the arc of high ZDR, while still wrapping into the knob of the hook, is less distinct. The central low r_{HV} and ZDR regions are comma-shaped, possibly as a result of debris and/or hail centrifuging (e.g., Dowell et al. 2005; Bluestein et al. 2007). At 2325, at 2km AGL, there is a large region of low ZDR well beyond the LRE and extending beyond the region of low r_{HV} . Within the low r_{HV} region there is a region exhibiting high r_{HV} values with only a slight increase in ZDR on the southwestern periphery. The high r_{HV} region overlaps the LRE and a region of high reflectivity to the south of the LRE (coincident with the slightly higher ZDR values). Based on the overlap of these fields, it is possible that smaller drops are present closer to the center of the circulation, while larger drops are present farther outward. Since these observations are from a height of approximately 2 km AGL, differential centrifuging and/or fall-out may be possible. KTLX observations near this time do not resolve these fine-scale details.

2.3 Rapid-Scan DOW observations of the tornado

⁴ Three-degree elevation scans are used because of partial beam blockage below that level. The Rapid-Scan DOW deployed at a site with minimal blockage, so even 0.5-degree elevation scans are usable.

RSDOW data collection, commencing after 2317:30, permitted study of even finer spatial and temporal scale evolution of velocity structures and the resolution of rapid changes in reflectivity features identified using dual-polarization data from DOW6. The large circulation and the interior vortex move rapidly eastward, crossing US-81 at a speed, $V_p \sim 25\text{m/s}$, comparable to the highest speeds ever documented by DOW radar observations, while the diameter of the interior sub-vortex increases from $DX_{\text{max}} = 150\text{m}$ to 350m . (This high V_p likely contributed to injuries among a media team, discussed below.). At 2317:38-2318:48, two comparable intensity circulations are evident, one inside the other, with diameters between maximum inbound and outbound winds, $D \sim 2000\text{m}$ and $\sim 150\text{m}$, similar to structures observed before (e.g., Kellerville, Texas (1995) and Harper, Kansas (2004); WK13)(Fig. 4). The larger circulation is best described as a large tornado/MVMC with a single (at this time) embedded sub-vortex following the nomenclature of WK13⁵. Additional vortices, especially prominent from 2318:48-2321:19, external to the primary circulation move towards it from the northwest and are ingested in a pattern similar to that observed in the Seward, Kansas (2008) and Oklaunion, Oklahoma (2000) tornadoes (WK13).

An important structural change occurs after 2320; the interior sub-vortex, which was nearly concentric with the larger tornado/MVMC, and moving with a similar V_p , is displaced. Additional vortices are also more apparent. Some of these vortices are associated with individual LREs and DREs (Fig. 5). The most intense vortex begins a trochoidal, sometimes prolate cycloidal⁶, motion about the larger

⁵ Alternately, the interior sub-vortex (sub-vortices) could be described as distinct tornado (tornadoes) embedded in a mesocyclone. However, then the width of damage caused by each of these tornadoes (as opposed to damage caused by the mesocyclone) would be $< 1\text{km}$. Also, while one sub-vortex is persistent, others are transient, and sometimes up to several are observed simultaneously. So, if the sub-vortices are described as tornadoes, then it would follow that this event comprised several (at least) individual small to moderate sized tornadoes.

⁶ True trochoids/cycloids are created by tracing lines created by points on non-slipping wheels. Most tornadoes, however, have peak tangential velocities, $V_t > V_p$, analogous to slipping wheels. Since the structure of the large tornado/MVMC is evolving, and the tornado is moving in curved path, possibly revolving about a larger circulation, the

circulation (Fig. 6), possibly similar to what was observed by a DOW in the Geary (2004) tornado/MVMC (WK13). The period between the apices of the retrograde loops at 2321:31, 2323:46, (and, by extrapolation, as the vortex becomes difficult to track at about 2326) was approximately 130 s. The sub-vortex becomes nearly stationary at the northwest extreme of the loops and moves at speeds of up to 79 m/s (the fastest ever documented) on the southeastern side of the larger tornado. Very approximately, these speeds and looping period would be consistent with revolving about a larger vortex at a radius of 750-1000m at a speed of $\sim 30\text{-}40\text{m/s}$.

Doppler velocities $> 115\text{ m/s}$ are observed in the sub-vortex just after 2326 while the vortex is moving at an appreciable angle across the RSDOW radar's beams. If axisymmetry and a simple Rankine-type profile are assumed and an assumed component of the very large but unobserved V_p of the sub-vortex is vectorially added (following Wurman et al. 2007a, where only $\sim 1\text{m/s}$ was added), peak V_g in this vortex ranges from 130-150 m/s, which is comparable to the highest ever reported. However, three factors complicate this comparison: 1. The current measurements are $\sim 100\text{m}$ AGL, adding great uncertainty concerning how to reduce to near ground levels (say 10m AGL), 2. There is uncertainty in the extremely high V_p of the sub-vortex and its angle relative to the DOW beams, and 3. The duration of the highest DOW-measured winds corresponds to $\ll 1\text{s}$ wind gusts over any fixed location (Fig. 7). Even if peak $V_g(100\text{m AGL}) = 140\text{m/s}$ in a small, extremely rapidly moving sub-vortex, a stationary observer/structure even at that height would only experience $V_g > 130\text{ m s}^{-1}$ for $\sim 0.5\text{s}$, much less than the 3s duration typically used when quantifying wind impacts. The 3s average V_g caused by this sub-vortex would be $< 100\text{m/s}$, depending mostly on the intensity of the surrounding flow, not the peak V_g in the sub-vortex.

The width of the MVMC, defined by a region enclosing DOW-measured $V_g > 30\text{m/s}$ (or, alternately, 50m/s), representing wind speeds potentially capable of causing marginal or substantial damage, but excluding the large rear-flank-downdraft to the south of the tornado,

prolate cycloidal description of the path of the sub-vortex is qualitative.

DX_{30} (DX_{50}), increased rapidly from 1.4km(0.6km) at 2317 to a maximum of 7km(5km) near 2319 (Fig. 5) perhaps the widest ever documented⁷. By comparison, Wurman (2002) reported $DX_{max}=1.6$ km and $DX_{30}=4.5$ km in the Mulhall, Oklahoma (1999) tornado and WK13 documented $DX_{max}\sim 2$ km in two tornadoes. Notably, however, dual-polarization evidence of debris from fine-scale DOW data below 1 km AGL is limited to a much smaller region, less than 2x3 km (Fig. 3), corresponding most closely to DX_{max} , not DX_{50} suggesting that substantial production and/or lofting of debris is not occurring throughout the entire region enclosed by DX_{50} .

After 2325, the tornado/MVMC contracts and exhibits a multiple-vortex structure with several comparable intensity sub-vortices, more typical of Mulhall (1999) (Wurman 2002; Lee and Wurman 2004)(Fig. 5). While this is the first time that this particular evolution, from interior near-center sub-vortex to offset vortex to multiple comparable intensity vortices, has been documented, a range of MVMC evolutions have been observed previously, for example in Quinter, Kansas (2008)(WK13) where a singlet tornado evolved into an MVMC which then evolved back into a singlet tornado. The El Reno tornado moves northward, then becomes nearly stationary near I-40 for ~400s from 2328-2335, then moves eastward for several minutes until becoming nearly stationary or looping again while dissipating at 2345 suggestive that the larger circulation is itself moving in a trochoidal fashion inside a larger mesocyclone.

In addition to the complex and changing structure of the main tornado/MVMC, the parent thunderstorm spawned a rare strong anticyclonic tornado with peak $V_g=65$ m/s at ~2328 in the anticyclonic shear zone to the southeast of the main tornado/MVMC, exhibiting multiple-vortex structure and a dual-polarimetric debris signature and lasting until ~2343 (Fig. 8). The

sub-vortices are associated with LREs and perturbations in the DS of the tornado in a region exhibiting reduced ZDR and r_{HV} . To the authors' knowledge, this is the first ever time sub-vortices and DSs have been documented in an anticyclonic tornado. DOW data show that the second anti-cyclonic velocity couplet observed by both KTLX and DOWs did not extend to near the ground (< 100 m AGL).

2.4 Tornado Impacts Storm Chasing Teams

The vehicle operated by Tim Samaras, his son Paul Samaras, and Carl Young was discovered at approximately 35.4790 N and 97.9014 W, about 30m east of the intersection of Reuters Road/10th Street and Radio Road (Fig. 6,9). The vehicle can be observed at 2122:15 in a video collected by a storm chaser (Dan Robinson) travelling east on Reuters Road, east of Alfadale Road. When impacted by the tornado, the vehicle was located approximately 530 m west of the intersection of Reuters and Radio road, near where Reuters Road crosses over an intermittent stream. The trunk contents were found just south of this location. Based on debris locations, the inferred path of the vehicle is southward, eastward, and then east-northeastward to its resting place. The vehicle was destroyed and the researchers were killed (obituary: Economist 2013.)

Although the El Reno tornado was exceptional with respect to both size and intensity, Samaras had extensive experience deploying instrumentation in and near tornadoes, some of which were large, intense and complex in structure (Lee et al. 2004;2011; Wurman and Samaras 2004; Karstens et al. 2010). Since the members of this team died despite having experienced leadership, the circumstances leading to their deaths have particular importance to tornado researchers as well as recreational, media, and storm-tour chasers, whose missions bring them near tornadoes.

It is likely that many details of the events leading to the deaths of the Samaras team will remain unknown. However, with the aid of DOW data and video documentation, it is possible to reconstruct some of the key details of the meteorological conditions leading to the destruction of their vehicle and speculate why this team fell victim. Visible in the video, the Samaras team drove eastward on Reuters Road

⁷ Tornado width is poorly and subjectively defined. It is variously described as the distance across different Doppler velocity thresholds, the distance perpendicular to the track in which damage is documented, the maximum width, in any direction, of winds over a threshold, and the diameter of the core flow region. DX_{50} in this tornado exceeds that observed by DOWs in any other tornado. Maximum DOW-measured cross-track width is observed earlier, at about 2319 (Fig. 1). The extreme cross-track width of observed damage may have been enhanced by damage caused by external vortices.

and they penetrated the ~2km diameter core flow region of the large tornado/MVMC, just behind the Robinson vehicle, at about 2321-2322. Conditions at the north edge of and inside this circulation were quite harsh, as evident in the video, but not nearly as severe as on the south/strong side. The Robinson vehicle moved eastward at approximately 20m/s, but the Samaras vehicle is seen to fall behind. One or more condensation funnels, likely associated with the DOW-observed sub-vortex, are visible to the south of the road. In the video, the Samaras vehicle's headlights are last seen to the west of Radio Road at 2322:15.

The above-described sub-vortex transcribes a loop, becoming nearly stationary near 35.473 N, 97.923 W at 2321:31, then moves rapidly around the south side of the tornado with V_p averaging 25m/s, peaking at 36m/s, while broadening, from 2321:56 to 2322:44, then contracts and re-intensifies at 2322:59 (Figs. 7,10), approximately 470m to the south of Reuters Road. Peak V_g exceeds 81m/s as the sub-vortex, with $DX_{max}=90-230m$, moves toward the north, then northwest, becoming nearly stationary over Reuters Road from 2323:35-2323:57, centered just to the east of the inferred starting position of the Samaras vehicle (and the location where the trunk contents were found). A distinct debris ring echo (DRE) surrounds the Samaras vehicle's location. The diameter of the debris ring grows at ~2-3m/s from ~600m to ~800m from 2323:32-2323:13. Subsequently, the vortex resumes its rapid eastward motion, crossing Radio Road, moving northeast then north with V_p as high as 79m/s.

The last sighting of the Samaras vehicle's headlights, the location of the trunk contents, and the location where the vehicle was discovered are consistent with it being transported initially southward by strong northerly flow on the west side of the sub-vortex, then roughly eastward about the south side of the vortex as the vortex remained quasi-stationary for about 20s. The vehicle could have covered the approximately 600m path from starting to ending location during the 20s period that the sub-vortex was quasi-stationary, if the vehicle was transported at a plausible speed of about 30 m/s (recalling that $V_g > 70m/s$ on the south side of the sub-vortex during this period).

As the larger tornado/MVMC moved northeastward, two additional sub-vortices

passed near these locations. One passed to the south of Reuters Road, likely causing strong easterly winds over the road, inconsistent with the eastward transport of the vehicle. The other grazed the road, and may not have crossed over the intersection with Radio Road. The movement and evolution of the sub-vortex that was quasi-stationary over Reuters Road just before 2324 is the most consistent with it transporting the vehicle.

A Weather Channel vehicle driving southward on US-81, penetrated into the tornado/MVMC in an attempt to traverse to the southern side of the tornadic region. It was impacted and damaged by the small central sub-vortex portion of the tornado/MVMC as the center of both the larger and smaller circulations crossed US-81, moving rapidly east-northward, with $V_p \sim 25m/s$ (Fig. 9). The high V_p likely contributed to its impacting the media vehicle. Westerly winds on the southern side of the central vortex exceeded 83m/s at 120 m AGL and transported the vehicle to the east side of US-81, injuring the occupants.

The exceptionally large, complex and intense El Reno tornado/MVMC of 31-May-2013 killed eight people, including an experienced storm chasing team which was likely impacted by an almost impossible to (visually) predict sub-vortex within the larger circulation. Both the Samaras and Weather Channel vehicles penetrated within the DX_{max} , i.e. within the RMW, of the large tornado/MVMC circulation. Both penetrated the weak side of the MVMC/tornado, so may have been unaware that they were inside.

However, while the Samaras team was inside the tornado/MVMC, already in poor conditions and surrounded by even more intense winds, an interior sub-vortex, which transcribed a prolate cycloid path for the preceding ~200s, intensified just 500 m to their south-southeast, moved north-northwestward, becoming nearly stationary just east of their vehicle. With only 30s potential warning, possibly low visibility inside the RMW of the larger MVMC/tornado, and the anomalous and rapidly-changing direction of movement of the sub-vortex, it is likely that no clear direction to safety was apparent. The Weather Channel team penetrated the larger tornado/MVMC, experiencing only moderately severe winds, but

then was impacted by a very rapidly moving interior sub-vortex.

Though it was an interior sub-vortex that impacted both the Samaras and Weather Channel teams, some more simply structured singlet tornadoes exhibit highly anomalous tracks, adding to the hazard they pose to the public and those in pursuit. This tornado/MVMC became nearly stationary near Interstate 40 from 2329-2335, moving <500m during 300s, a $V_p < 2\text{m/s}$, then abruptly resumed a more normal eastward motion. This type of motion is typical of maturing tornadoes revolving about mesocyclonic circulations.

2.5 Summary

A large and violent tornado/multiple vortex mesocyclone (MVMC) / tornado tracked east and northeastward near El Reno, Oklahoma on 31-May-2013, causing eight fatalities, including storm-chasers/researchers attempting to deploy in-situ instrumentation. Sub-vortices moved within and near the MVMC, some in trochoidal-like patterns, with ground-relative translational velocities ranging from 0-79m/s, the fastest ever documented. Doppler On Wheels (DOW) measurements in one of these sub-vortices exceeded 115m/s at 114m AGL. With assumptions concerning radar-unobserved components of the velocity, peak wind speeds of 130-145m/s are implied, comparable to the strongest ever measured. Only Enhanced Fujita Scale-3 (EF-3) damage was documented, likely due to a paucity of well-built structures and the most intense winds being confined to small, rapidly moving, sub-vortices resulting in only sub-second gusts. The region enclosing the maximum winds of the tornado/MVMC extended ~2km. DOW-measured winds >50m/s (>30m/s) extended far outward from the radius of maximum winds (RMW) extending >5km(7km), comparable to the widest ever documented. A strong multiple-vortex anticyclonic tornado with dual-polarization debris signatures is documented.

3. The Bennington, Kansas tornado

A striking example of unpredictable tornado path was exhibited by a violent tornado occurring near Bennington, Kansas on 28-May-2013. The tornado persisted for over 4000s; near-surface Doppler winds reached 118m/s, a double gust front structure (Wurman et al.

2007b, Marquis et al. 2008; Kosiba et al. 2013) was observed, and a discontinuous DRE developed as the tornado crossed over a region with trees (Fig 11). The forward speed of the tornado typically was quite slow, <0.3 m/s over 300s, and the track looped back on itself. Observers “behind” the tornado remained at considerable risk.

4. The Rozel, Kansas and Wichita, Kansas tornadoes

The DOWs also obtained data in the EF-4-rated tornado on 18 May near Rozel, Kansas and EF-2-rated tornado on 19 May near Wichita, Kansas⁸ (Fig. 11). No Pods were deployed in either of these tornadoes, but fine-scale dual-Doppler opportunities may exist.

5. Conclusions

What role can technology play in enhancing the safety of missions near tornadoes? Research teams who deploy in-situ Tornado Pods during the Radar Observations of Tornadoes and Thunderstorms Experiment (ROTATE, Wurman 2008) operate under the safety umbrella provided by real-time DOW mapping of tornado winds updating every 7s, which provides detailed information concerning tornado intensity, size, multiple-vortex structure and changing path. DOW real-time scanning was critical to team safety when the DOW was inside the Geary, Oklahoma tornado/MVMC, allowing the DOW to avoid an optically invisible interior sub-vortex. The ROTATE science team navigated outside the DX_{max} of the after-dark and invisible tornado/MVMC in Seward, Kansas using DOW-provided information. ROTATE Tornado Pod deployment missions are aborted if real-time DOW radar coverage is lost. *Critically, the ROTATE team aborted their attempt to deploy Tornado Pods in the El Reno tornado when real-time DOW data revealed a violent, complex, and large circulation with an additional anticyclonic tornado to the south, and aborted their mission on the Bennington, Kansas tornado, due to lack of track predictability.*

A few storm chasers have employed armored vehicles to provide safety inside DX_{max} (e.g., the Tornado Intercept Vehicle (TIV), Wurman et al. 2007; Wurman et al. 2013).

⁸ Both of these EF-Scale ratings may be preliminary, and were DOW-influenced.

These likely provide substantial added protection, but none are engineered rigorously against the most intense winds or debris hazards. DOWs have armored cabins and low centers of gravity providing protection against moderate intensity winds and debris typical of some tornadoes and most hurricanes, but Tornado Pod deployment trucks are not armored. The Samaras team's Chevy Cobalt was not especially heavy or armored, likely adding to its vulnerability once the team penetrated the region inside DX_{\max} of the tornado/MVMC.

Chasing tornadoes appears to be a generally low-risk activity based on the rarity of injuries and fatalities. However, without access to real-time mobile radar data, storm chasers, particularly those attempting to deploy instrumentation inside tornadoes or film especially close to tornadoes, may inadvertently penetrate the RMW of large tornadoes/MVMCs and find themselves particularly vulnerable to intense winds contained in interior sub-vortices such as those documented in Geary (2004) and El Reno (2013). The fatal and non-fatal incidents documented here should provide a cautionary note to those pursuing activities near tornadoes, with particular focus on the hazards of penetrating within the RMW of large tornadoes/MVMCs.

6. Acknowledgments

Thanks to the ROTATE-2013 crew. This analysis was supported by NSF-AGS-1211132 and the DOWs are supported by NSF-AGS-0734001.

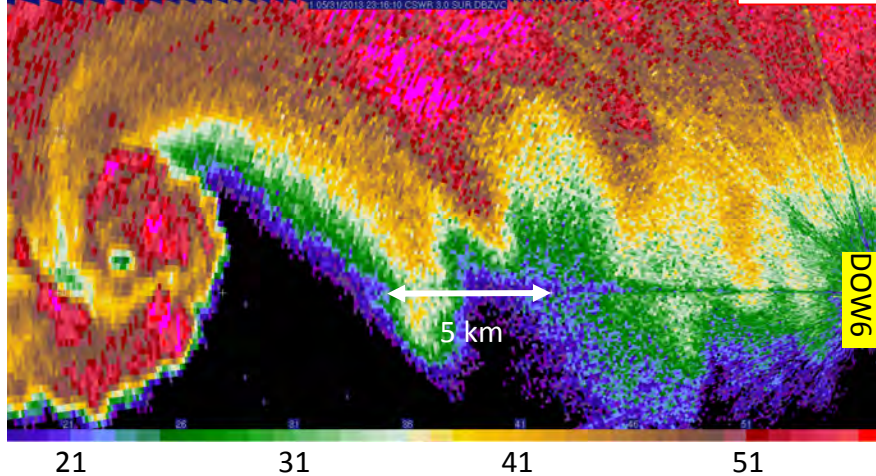
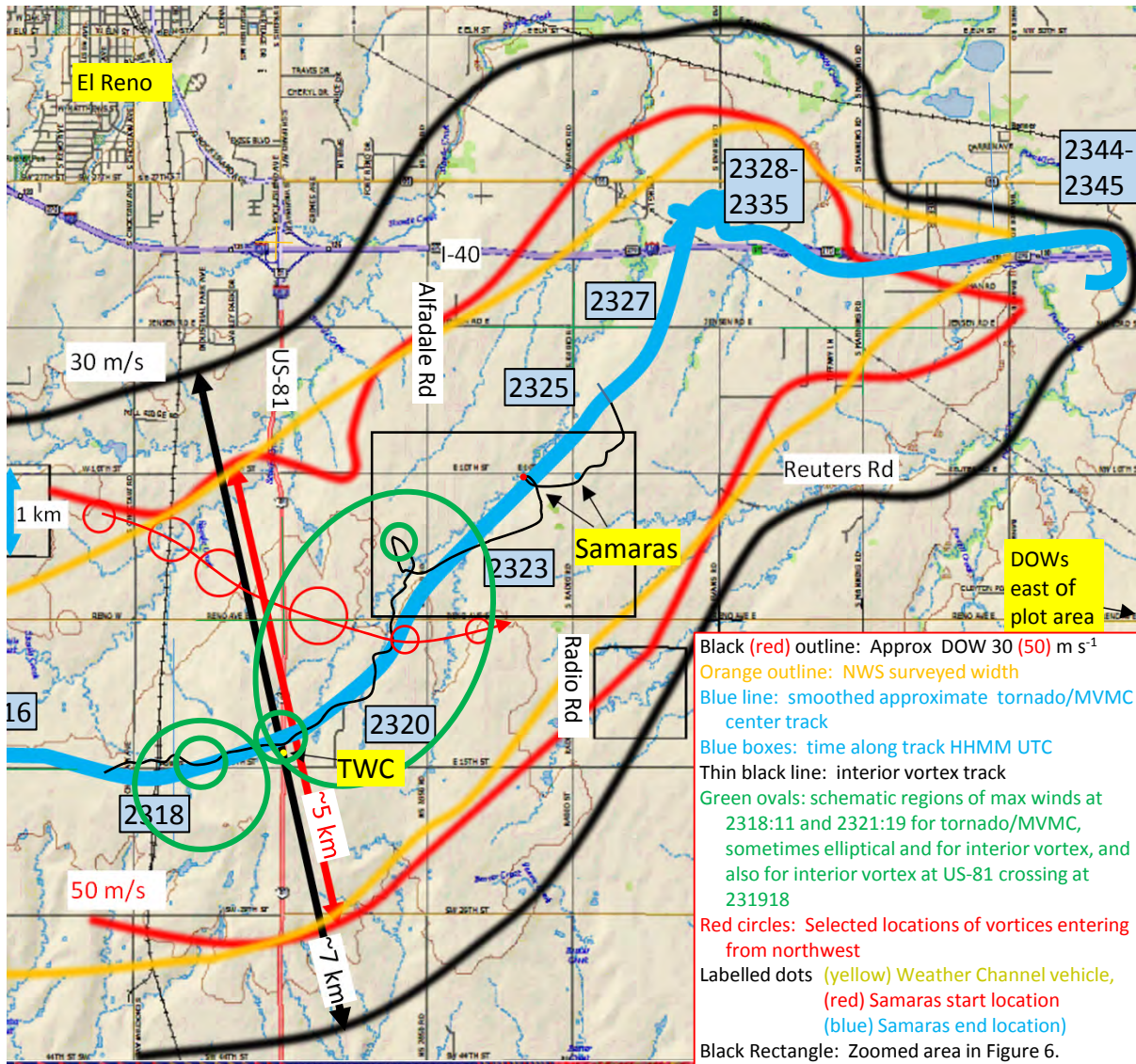


Figure 1. (top) Track of tornado/MVMC, internal sub-vortex impacting research team, and other vortices near El Reno, Oklahoma on 31 May 2013. Very wide path and complex and intense multiple vortex structure combined to make this tornado particularly hazardous.

(bottom) Reflectivity in the supercell thunderstorm as measured by DOW6 at 3 degrees, approximately 1 km AGL at 2316:10 UTC.

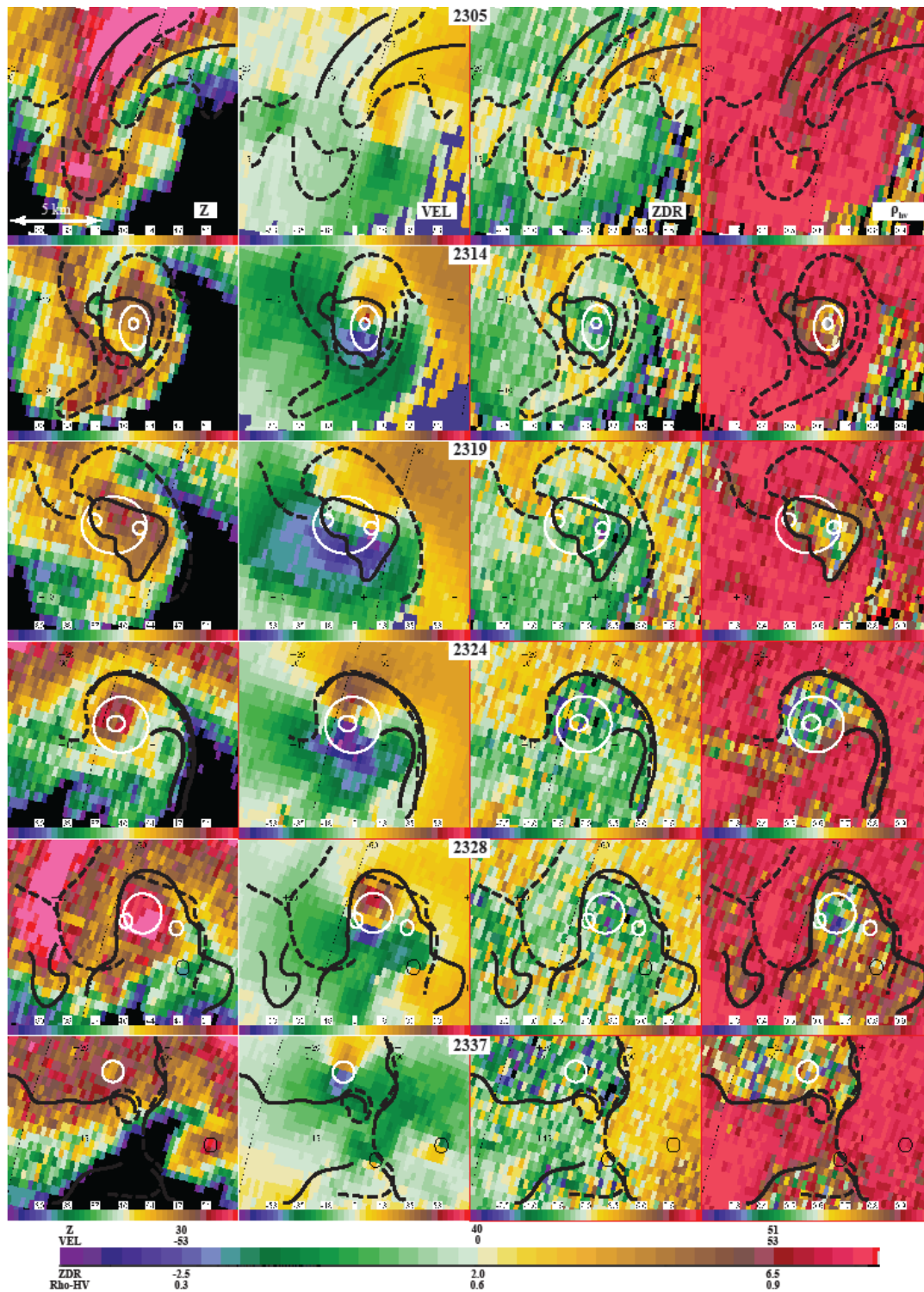


Figure 2. El Reno tornado and anticyclonic tornado as observed by KTLX. Columns from left to right: Reflectivity (Z), Doppler Velocity (VEL), Differential Reflectivity (ZDR), and the cross-correlation coefficient (ρ_{HV}). Prominent vortices, including the large tornado/MVMC, visible internal vortices are outlined in white. Anticyclonic vortices, one of which is a tornado, are in black. Stippled (Solid) black lines indicate interesting regions of high (low) ZDR (ρ_{HV}) field(s).

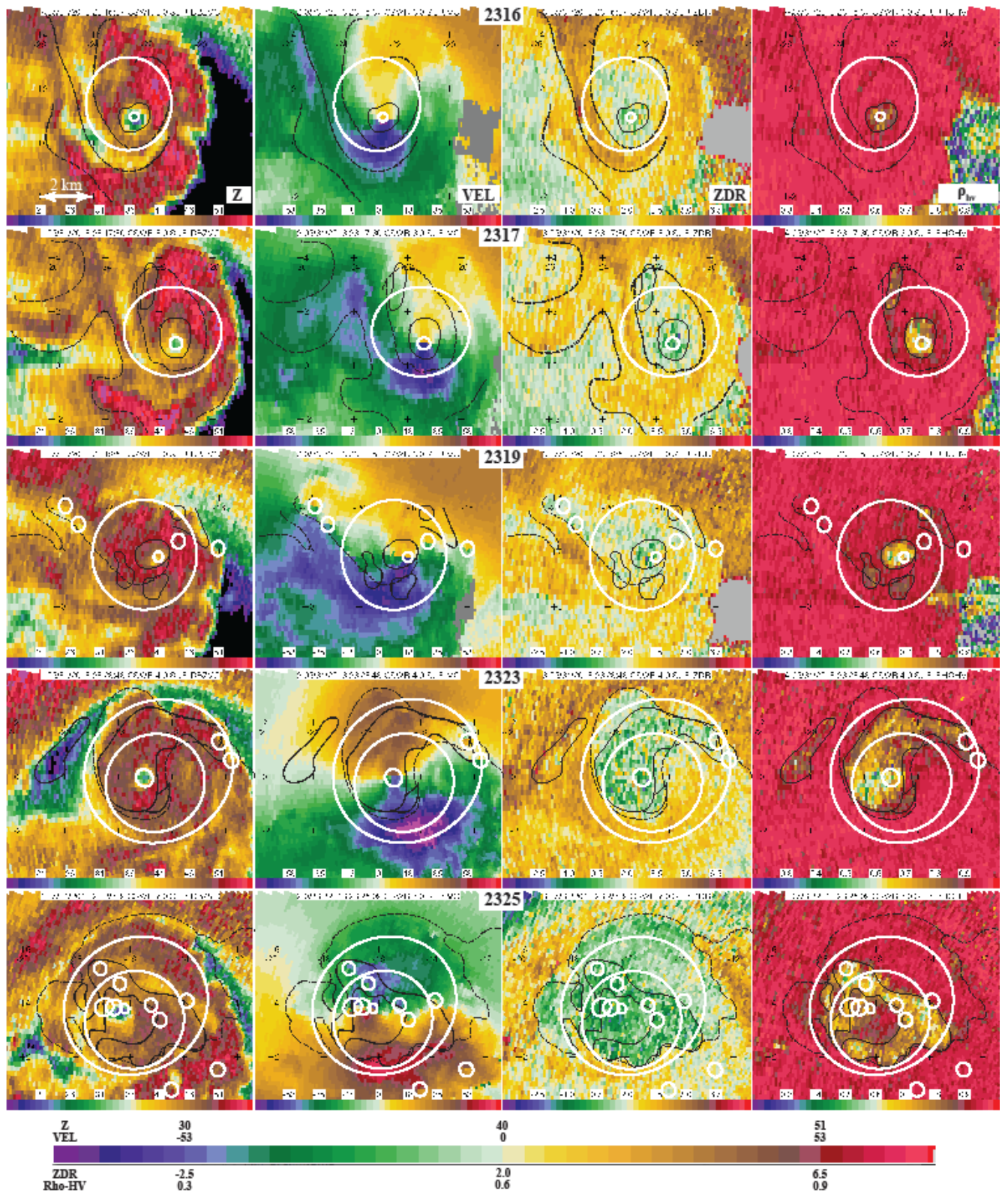


Figure 3. El Reno tornado and anticyclonic tornado as observed by DOW6. Columns from left to right: Reflectivity (Z), Doppler Velocity (VEL), Differential Reflectivity (ZDR), and the cross-correlation coefficient (ρ_{HV}). Prominent vortices, including the large tornado/MVMC, visible internal vortices are outlined in white. Stippled (Solid) black lines indicate interesting regions of high (low) ZDR (ρ_{HV}) field(s).

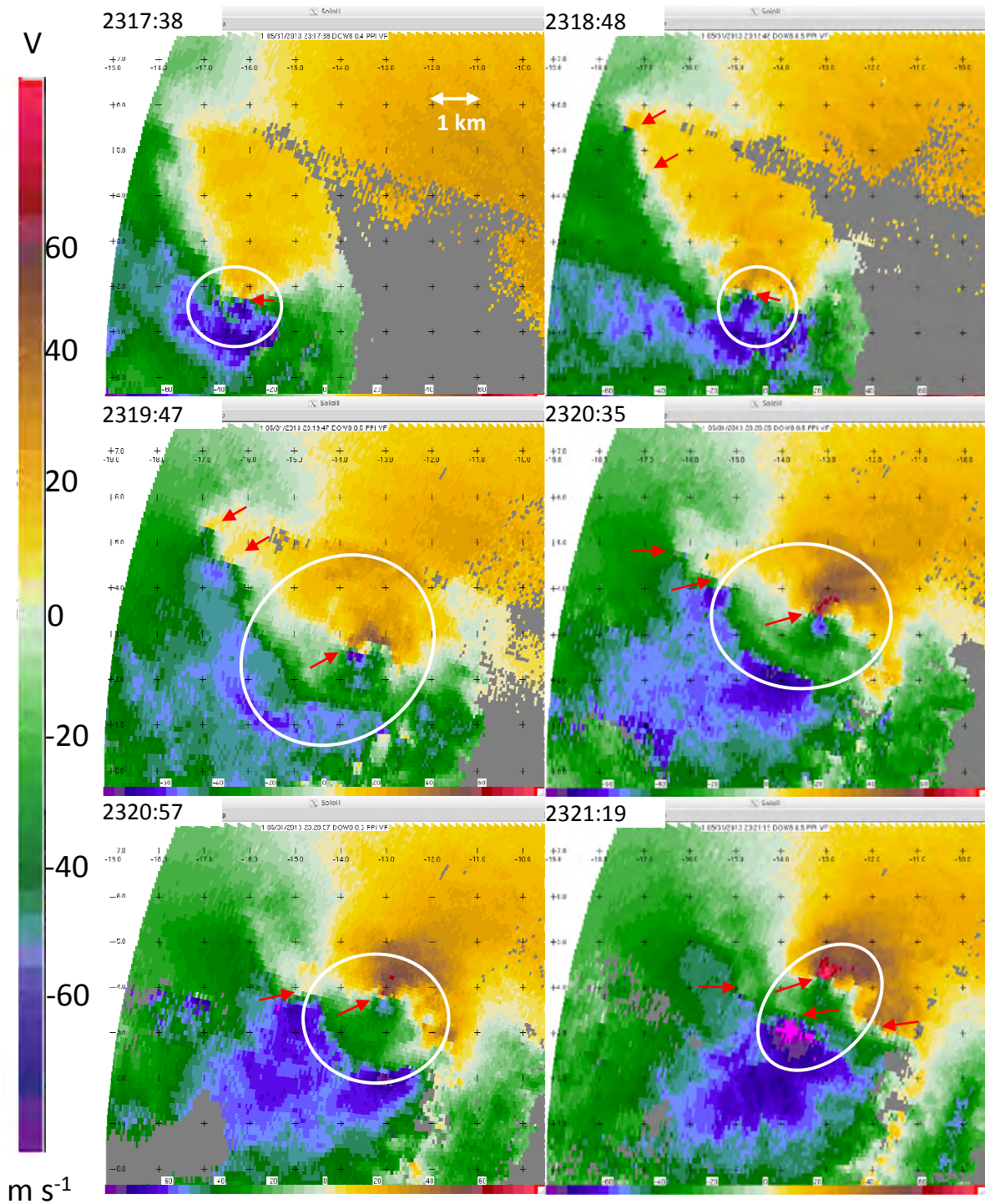


Figure 4: Evolution of the tornado/MCMV from 2317:38 to 2321:19 as observed by the RSDOW. White circles denote the larger scale vortex and the red arrows denote sub-vortices. After 2318, the winds associated with the larger-scale vortex are comparable to or larger than the interior sub-vortex. The region enclosing maximum winds of the MVMC is sometimes very elliptical.

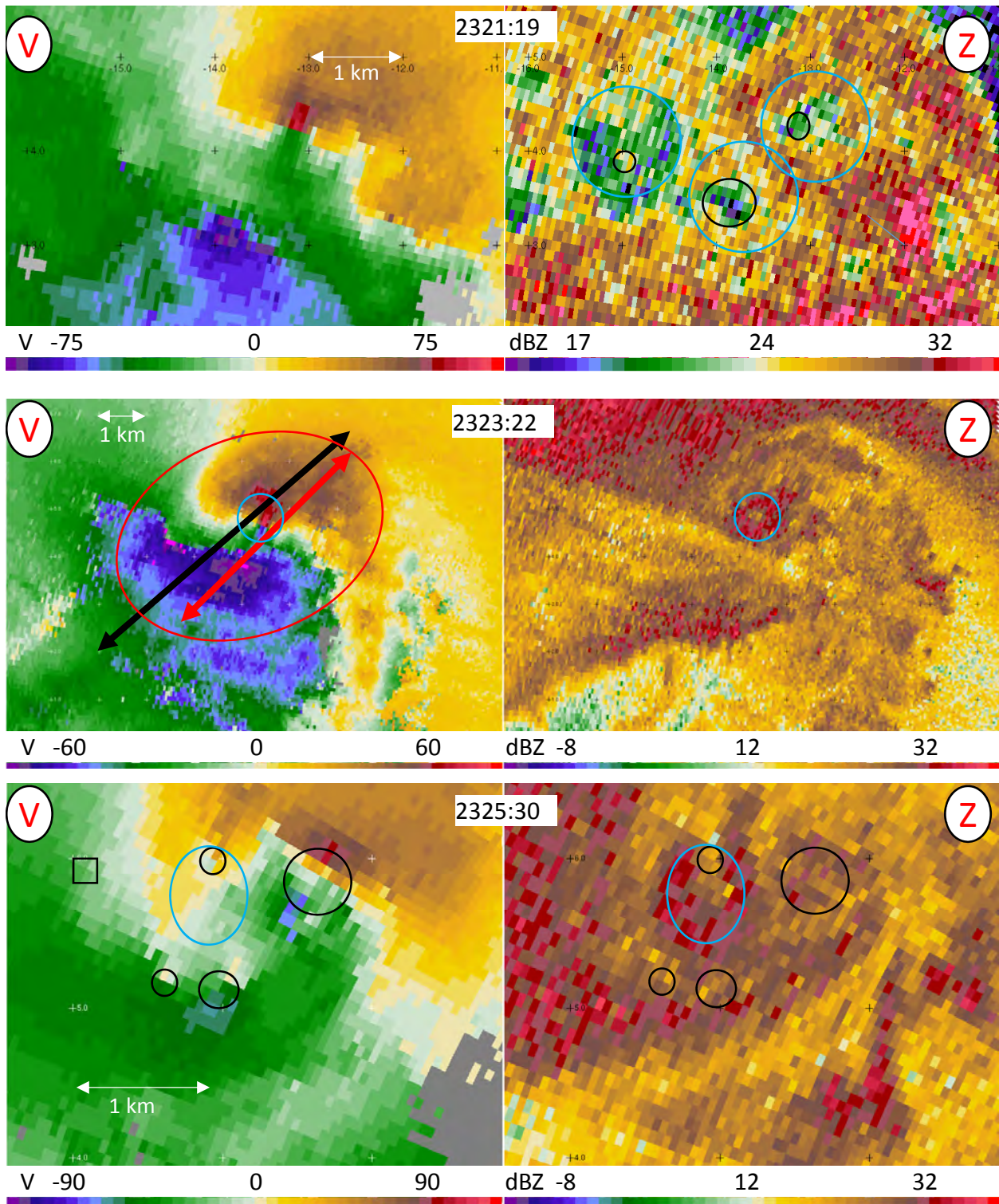


Figure 5. Doppler Velocity (left) and Reflectivity (right). (top) strong vortices, exterior vortex, with LRE and DS/DRE signatures (blue rings). (middle) Large along-track width of 30 m s⁻¹ and 50 m s⁻¹ radar winds, ~ 2km diameter circulation and strong interior vortex. Red oval delineates approximate region with inferred winds > 50 m s⁻¹. (bottom) several sub-vortices. Blue rings schematically illustrate debris ring echoes (DRE). Black rings denote velocity signatures of sub-vortices.

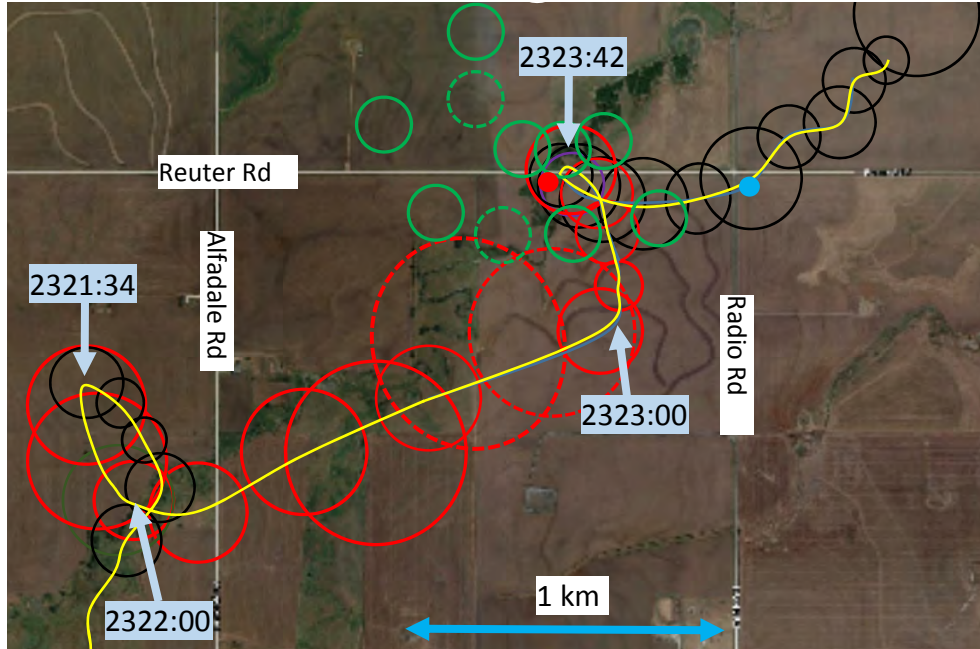


Figure 6. Smoothed track of interior sub-vortex as measured by the Rapid-Scan DOW. Yellow line is approximate center of circulation. Red and black circles delineate, at selected times, the approximate region enclosing the maximum tangential velocity, V_{tm} . Blue boxes label selected times along the track in HHMM:SS UTC. Red (blue) dots represent start (end) locations of the Samaras team's vehicle. Green circles delineate vortices impacting the same area shortly afterwards. The vortex executes a loop at 2321:34, moves rapidly east-northeastward from 2322:00 until 2323:00, then more slowly north-northwestward, becoming stationary over Reuters road and the vehicle, then moves east-northeastward again.

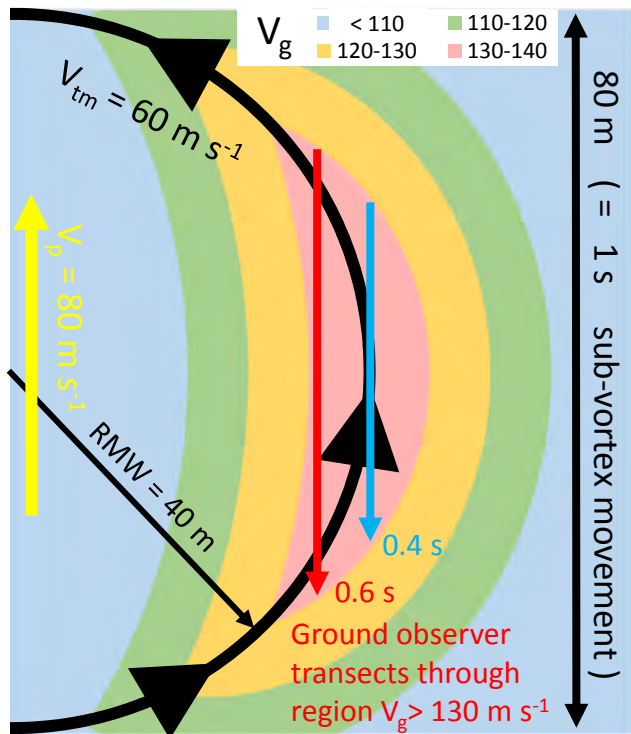


Figure 7. Schematic of strong V_g side of rapidly moving sub-vortex. Very fast $V_p = 80 \text{ m s}^{-1}$, adds to peak tangential winds $V_{tm} = 60 \text{ m s}^{-1}$, at and near the radius of maximum winds resulting in peak $V_g = 140 \text{ m s}^{-1}$. However, due to very fast V_p , the duration of $V_g > 130 \text{ m s}^{-1}$ over a stationary object or observer is $\leq 0.6 \text{ s}$.

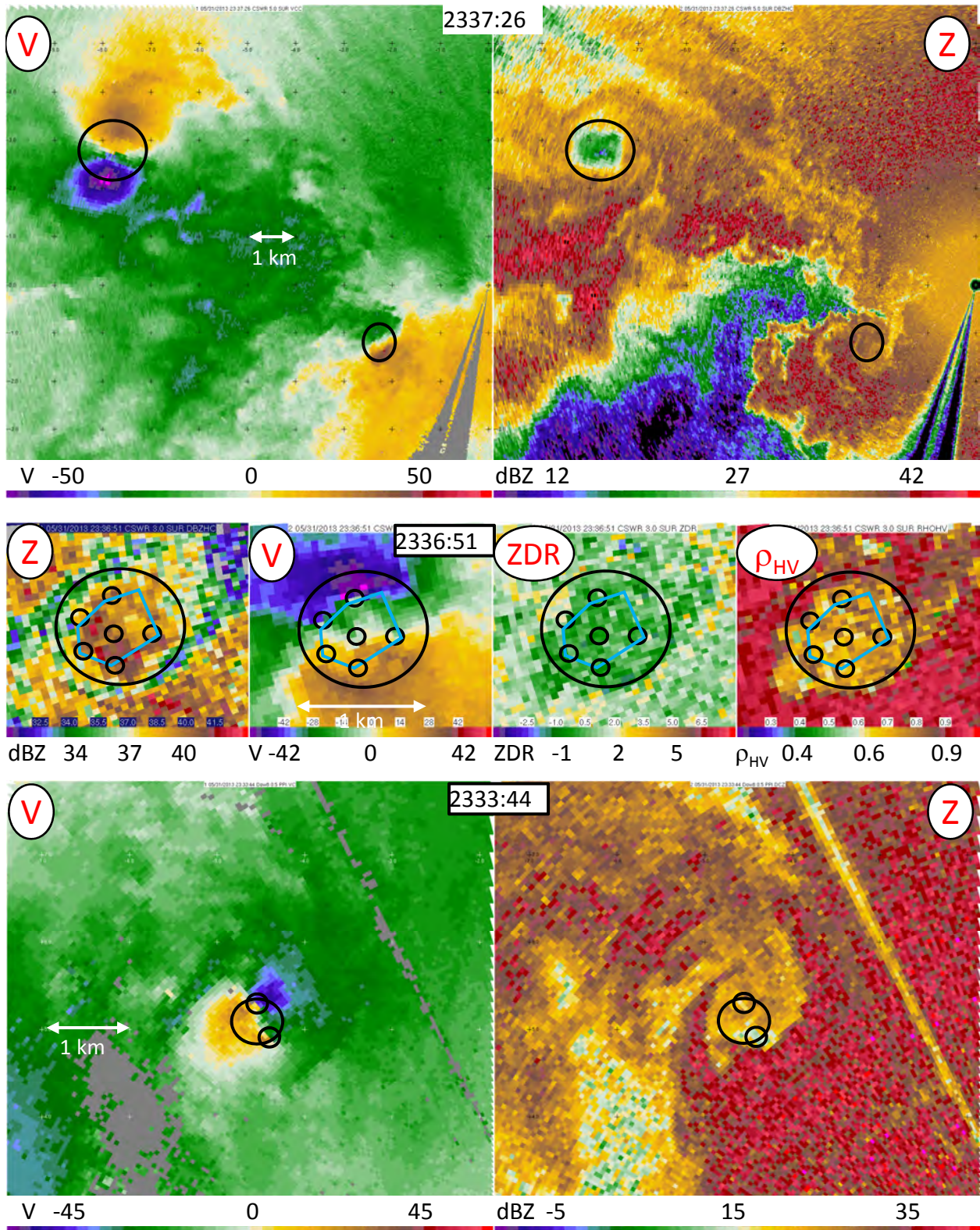


Figure 8. Anticyclonic Tornado (top) Doppler Velocity (left) and Reflectivity (right) in cyclonic and anticyclonic tornado. (middle) DOW6 Reflectivity, Velocity, ZDR, and ρ_{HV} . Blue polygon denotes quasi-polygonal debris ring echo (DRE) in region of reduced ZDR and ρ_{HV} . (bottom) Multiple vortex structure of the anticyclonic tornado is evident in both RSWDOW velocity and reflectivity fields.



Figure 9. Tim Samaras's (top two panels) and the Weather Channel (bottom panel) vehicles after they were transported by winds in the embedded sub-vortex inside the large tornado. Moderate damage to trees is evident.

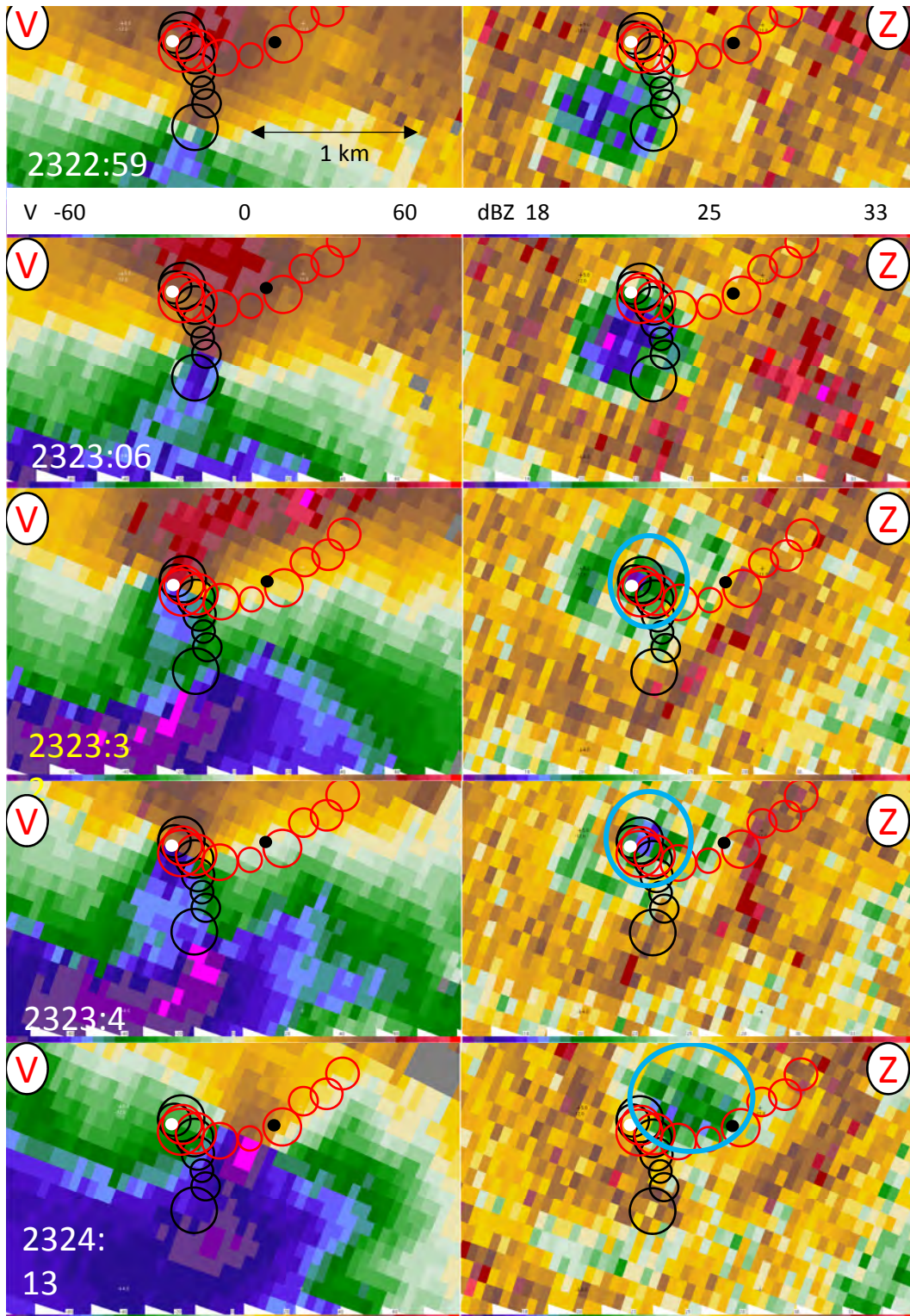


Figure 10. Doppler Velocity (left) and Reflectivity (right). DOW sweeps at selected times illustrating path of sub-vortex which impacted Samaras research team. Red and black rings are schematic indications of region enclosing maximum winds. Times are HHMM:SS UTC. Blue ring (right panels) annotates widening debris ring echo (DRE). White/Black dots are start/end location of vehicle. Beginning at ~2323:32, vehicle was transported south, then east about southern side of the sub-vortex.

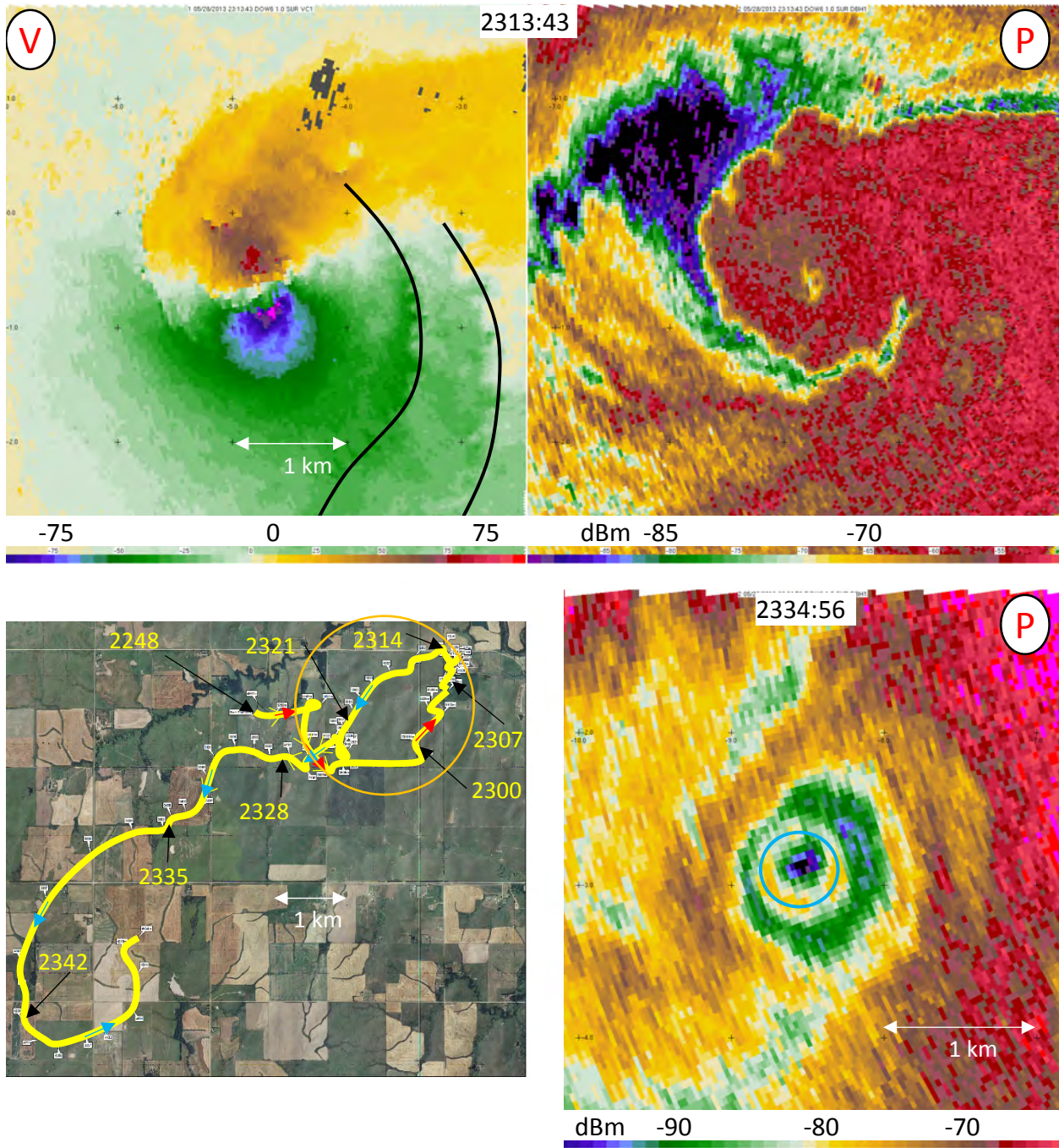
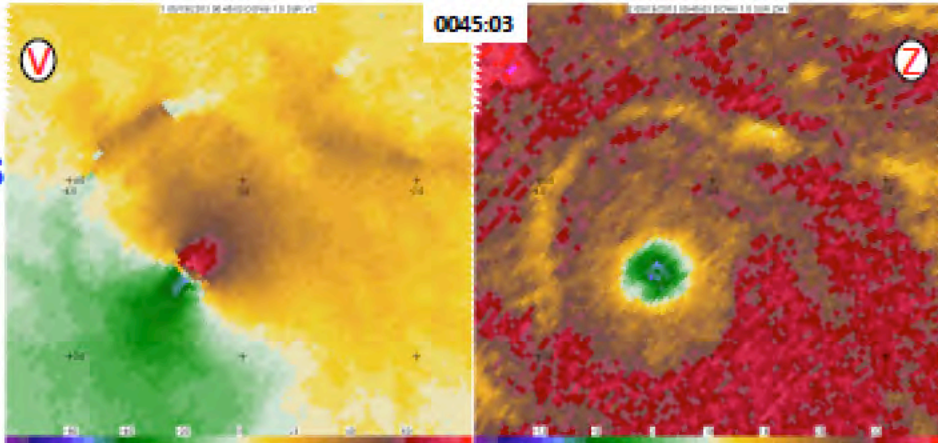


Figure 11. **(top)** Doppler Velocity (left) and Received Power (right) in Bennington, Kansas tornado on 28 May 2013. Winds exceeded 118 m s^{-1} at 47 m AGL. **(Bottom left)** looping track of tornado from 2247-2347 UTC. Tornado formed before 2247, but DOW-based locations are less precise since the DOW was in motion. Tornado was nearly stationary from 2308-2313, moving less than 80 m over 300 s, and traced multiple loops during that and other periods, remaining within a 2.5 km diameter circle (orange) for 2000 s. **(Bottom right)** Discontinuous debris ring echo (DRE) as tornado passes over region with trees.

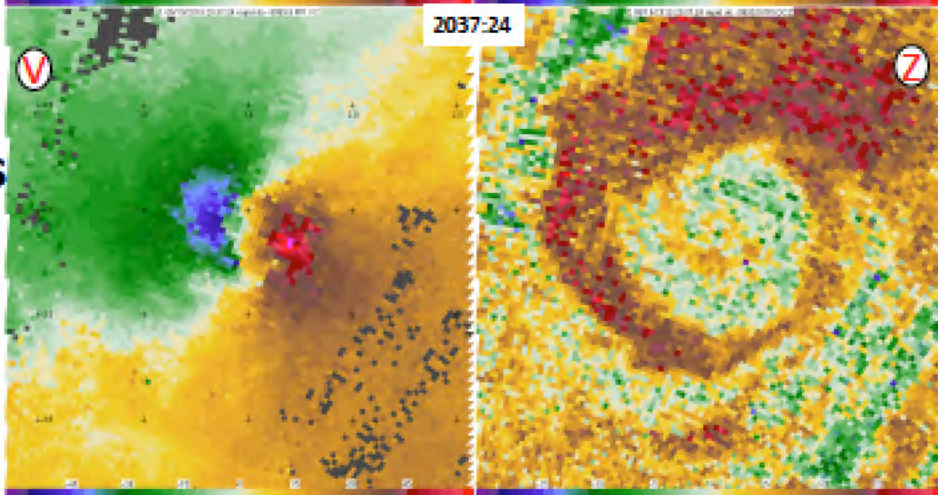
Rozel, KS: EF-4*

**DOW-Measured winds
of 78-83 m/s**



Wichita, KS: EF-2*

**DOW-Measured winds
of 60-64 m/s**



*DOW-Influenced Preliminary Ratings